FATIGUE CRACK PROPAGATION IN AN Fe$_3$Al BASED ALLOY TESTED AT ELEVATED TEMPERATURES

PETR HAUŠILD*, MIROSLAV KARLÍK, IVAN NEDBAL, JAKUB PRAHL

The fatigue fracture properties of the hot rolled Fe-28at.%Al intermetallic alloy with the addition of chromium and cerium were studied at elevated temperatures. The fatigue crack growth rate (ν-ΔK) curves were measured at 20, 300 and 500 °C. The alloy presents the best resistance against the fatigue crack growth at 300 °C, except for the low values of ΔK (< 24 MPa $\sqrt{\text{m}}$) for which the alloy has the lowest crack growth rate at 20 °C.

Fractographic analysis carried out on fracture surfaces of ruptured specimens revealed several failure mechanisms of crack propagation. The main fatigue crack growth mechanism at all studied temperatures is transgranular cleavage. The fatigue fracture surface shows varied micromorphology. Besides transgranular cleavage, transgranular quasi-cleavage facets, ductile fatigue striations and brittle striations were found.

In the zone of final (static) fracture, the material showed an increasing capacity of plastic deformation with increasing temperature. Fracture mechanism changed from transgranular cleavage at 20 °C to ductile dimpled fracture at 500 °C.

K e y   w o r d s: iron aluminides, fracture micromechanisms, fractography, fatigue crack growth

ŠÍŘENÍ ÚNAVOVÉ TRHLINY VE SLITINĚ NA BÁZI Fe$_3$Al PŘI ZKOUŠKÁCH ZA ZVÝŠENÝCH TEPLOT

Únavové chování intermetalické slitiny Fe-28at.%Al s příměsí chrómu a céru válcované za tepla bylo studováno při zvýšených teplotách. Závislost ν-ΔK byla naměřena při 20, 300 a 500 °C. Slitina vykázala nejvyšší únavovou odolnost při 300 °C s výjimkou nízkých hodnot ΔK (< 24 MPa $\sqrt{\text{m}}$), pro které měla nejnižší rychlost šíření únavové trhliny při 20 °C.

Czech Technical University in Prague, Faculty of Nuclear Sciences and Physical Engineering, Department of Materials, Trojanova 13, 120 00 Prague 2, Czech Republic

*   corresponding author, e-mail: hausild@kmat.fjfi.cvut.cz

Lomové plochy porušených těles vykazují různou mikromorfologii lomu. Fraktografická analýza určila jako hlavní mikromechanismus únavového lomu za všech studovaných teplot transkrystalické štěpení. Kromě transkrystalického štěpení byly nalezeny také transkrystalické kvazištěpné fasety, tvárné a štěpné striace.

V oblasti statického dolomu vykazoval materiál s rostoucí teplotou rostoucí schopnost plastické deformace. Došlo ke změně mikromechanismu lomu ze štěpného při 20 ℃ na tvárný důlkový lom při 500 ℃.

1.   Introduction

Iron aluminides based on Fe_3Al are potentially important structural materials for moderate and high temperature applications owing to their high specific strength, good wear resistance, superior corrosion resistance in oxidizing and sulfidizing atmospheres, low material cost, ease of fabrication, availability of raw materials and conservation of strategic elements [1]. They can replace steels and nickel based alloys in many special applications including heating elements, furnace fixtures, heat-exchanger piping, sintered porous gas-metal filters, automobile and other industrial valve components [2]. Possible applications are greatly limited by low room temperature ductility of these materials, resulting mainly from environmental hydrogen embrittlement [3] and a sharp decrease in yield strength above the $D0_3 \leftrightarrow B_2$ order-order transition at the temperature about 540 ℃. Therefore, research has been concentrated on improving room temperature (RT) ductility and high temperature (HT) creep strength and finally it has been shown, that sufficient engineering RT ductility of 10 to 20 % and tensile yield strength as high as 500 MPa at 600 ℃ can be reached through control of composition and microstructure [4]. Alloying elements such as Si, Ta, Zr, Mo, Ti, Hf, Nb and W have been shown to increase HT creep and tensile strength of Fe_3Al, usually at the expense of RT ductility [5]. Chromium increases RT ductility while it has almost no effect on strength [6]. Microalloying by cerium is beneficial both to HT strength and RT ductility [7]. Refinement of the grain size due to the addition of Zr, TiB_2 or Ce enhances the RT ductility. The effect of thermomechanical treatment is also important [8–10]. A more detailed description of the state of the art in the research of iron aluminides is given in a review by Stoloff [11]. The fatigue crack growth was measured on Fe-28Al-5at.%Cr alloy in air, oxygen and vacuum by Castagna and Stoloff [12] and Alven and Stoloff [13]. The same authors found a beneficial effect of Zr addition on the ductility and fatigue crack growth resistance of Fe-28Al-5at.%Cr alloy [14].

This paper reports fractographic analysis carried out on samples of Fe-28Al--3Cr-Ce (at.%) alloy fatigue tested in air at temperatures of 300 and 500 ℃ and compares it with the RT results obtained on the same alloy and specimen geometry [15].

2. Experimental details

An alloy with nominal composition of Fe-28Al-3Cr-Ce (at.%) was prepared by vacuum induction melting and casting. The ingot was hot rolled at 1100 °C to a plate 6 mm thick (reduction 75 %) and subsequently quenched into mineral oil. Results of the chemical analysis of the alloy are in Table 1. After machining by milling, the test specimens were annealed in air at 700 °C for 2 hours and quenched into mineral oil. The material was recovered, with elongated grains having $\sim 300\ \mu$m in the direction of rolling and $\sim 100\ \mu$m in the transverse direction. Static tensile test was carried out at temperatures 20, 300, and 500 °C on INSTRON 1186 testing machine equipped with a resistance-heated furnace. At each temperature, three cylindrical specimens having 3 mm in diameter and 20 mm gauge length were tested at the constant crosshead speed 2 mm/min (initial strain rate $1.6 \times 10^{-3}\,\mathrm{s^{-1}}$).

Fatigue crack growth experiments were performed on compact tension (CT) specimens of thickness $B = 5$ mm and width $W = 40$ mm. The notch was prepared by electro-discharge cutting using a wire 0.1 mm in diameter. The initial crack length a_0 was 8 mm (corresponding to $a_0/W = 0.2$). The fatigue crack propagated perpendicularly to the rolling direction. The specimens were loaded in tension at 20, 300 and 500 °C on a computer-controlled servohydraulic loading machine INOVA ZUZ 50 equipped with a resistance-heated furnace. The frequency of loading was 10 Hz, the stress ratio R was in the range from 0.05 to 0.1. The crack length during fatigue test was measured by (temperature independent) potential method at alternative current with the frequency of 4 Hz, using TECHLAB SRT-2K device, controlled by Fatigue Crack Growth Monitor software. Scanning electron microscope JEOL JSM 840A was used for the fractographic analysis. Micrographs were taken in the magnification range 10–20 000×.

T a b l e 1. Chemical composition of the alloy

	Al	Cr	Ce	C	Mn	Fe
(at.%)	28.99	3.19	0.008	0.157	0.026	Balance
(wt.%)	16.54	3.51	0.025	0.04	0.03	Balance

3. Results and discussion

3.1 Static mechanical properties

Table 2 gives average values of yield strength (YS), tensile strength (TS) and elongation measured at different temperatures. While at 20 and at 500 °C, the values of YS, TS and elongation are very similar (YS 375/324 MPa, TS 476/373 MPa, elongation 2.3/2.8 %), mechanical properties at 300 °C are different. The value of YS is slightly lower (244 MPa), TS is significantly higher (709 MPa), as well as the elongation (11.5 %). When compared to corresponding values of previously tested

materials of a similar composition and thermal treatment [16, 17], YS has a similar temperature dependence, as well as absolute values. On the other hand TS and elongation are roughly in agreement only for RT and 300 ℃. The drop of both of these values at 500 ℃ was not previously observed.

Table 2. Static mechanical properties of studied material

	20 ℃	300 ℃	500 ℃
0.2 yield strength [MPa]	375	244	324
Tensile strength [MPa]	476	709	473
Elongation [%]	2.3	11.5	2.8

3.2 Fatigue crack growth

The crack length a was measured during the fatigue tests as a function of elapsed number of loading cycles N. The fatigue crack growth rate $v = \mathrm{d}a/\mathrm{d}N$, determined by the secant method, is plotted in Fig. 1 as a function of stress intensity factor range ΔK (calculated for the corresponding crack length a).

The slope in ν-ΔK plot (exponent in Paris equation) is about four times higher at RT (~ 7.8) than at 300 ℃ (~ 1.9). For low $\Delta K (< 24$ MPa $\sqrt{\mathrm{m}}$) the alloy has the highest resistance against the fatigue crack growth (lowest crack growth rate) at RT. For $\Delta K > 24$ MPa $\sqrt{\mathrm{m}}$ the ν-ΔK curves obtained at RT and at 300 ℃ intersect (due to the higher Paris exponent at RT) and the crack growth rate becomes higher at RT than at 300 ℃. At 500 ℃ the slope in ν-ΔK plot remains practically the same as at 300 ℃ but the curve is shifted towards the higher crack growth rate values. The crack growth rate is about 1.5 order of magnitude higher at 500 ℃ than at 300 ℃ (for the same values of ΔK).

Lower resistance against the fatigue crack growth at 300 ℃ than at RT for low values of ΔK is probably due to lower YS noted in tensile tests (easier crack initiation). On the other hand for higher values of ΔK, an increase of plastic deformation capacity (together with higher TS) at 300 ℃ makes cleavage more difficult with consequent lower crack growth rate.

3.3 Fractography

The morphology of fatigue fracture surface is shown in Figure 2. The fracture surfaces were rugged and consisted of facets different in arrangement, size and micromorphology. The predominant fractographic feature is transgranular cleavage. Practically negligible changes of overall morphology character of fatigue fracture surfaces were found with increasing crack length (i.e. with increasing stress intensity factor), or with increasing temperature.
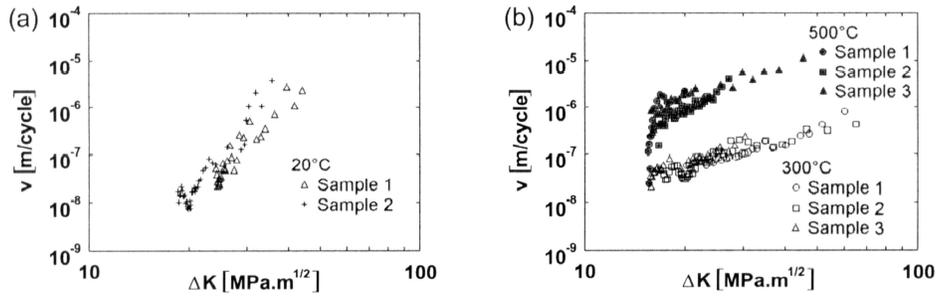
Fig. 1. Fatigue crack growth curves at room temperature (a), and at elevated
temperatures (b).

Fractographic observation pointed out the influence of microstructure on the micromorphology of fracture surface. Figure 3 shows the interaction of the fatigue crack with dislocation networks in recovered microstructure.

Besides transgranular cleavage, other types of facets were also found: Transgranular quasi-cleavage facets, ductile dimpled rupture, intergranular decohesion, ductile fatigue striations and brittle striations resulting from cyclic cleavage (Fig. 4). The fields of striations were typically formed on the small tilted areas connecting the large cleavage facets.

Common fatigue striations (Fig. 5) formed by the classical Lairds mechanism were found only exceptionally (most of them were observed at 300 °C). These striations are ductile, i.e. the relief of individual striations shows the signs of local plastic deformation. A detailed study of ductile striations was carried out by the technique of matching surfaces [13].

Some facets are covered by brittle striations exhibiting only very low local plastic deformation (Fig. 6). The character of these striations did not significantly change with increasing crack length. The local growth direction (given by the normal to the striation lines) was often perpendicular to the main crack growth direction, i.e. from the centre to the lateral faces of specimen. The spacing between the neighbouring striations varied from 0.1 to 5 μm frequently even in the range of one striations patch. In some cases, the striations with spacing smaller than expected (i.e. corresponding to the lower crack growth rate) were found in the zones situated close to the end of fatigue crack, where the macroscopic (measured) crack growth rate was very high and the fatigue life was practically spent. These striation fields containing facets could eventually be created ahead of the actual main crack front and they could subsequently be connected by the fast propagating cleavage facets. Obviously, the brittle striation spacing cannot be used for the crack growth rate estimation (as e.g. in Ref. [14]), since the local crack growth rate given by the striation spacing is not representative for the growth rate of the main crack front.

The main influence of temperature was observed in the zone of final (static) fracture (Fig. 2). The material showed an increasing capacity of plastic deformation

RT   300°C   500°C
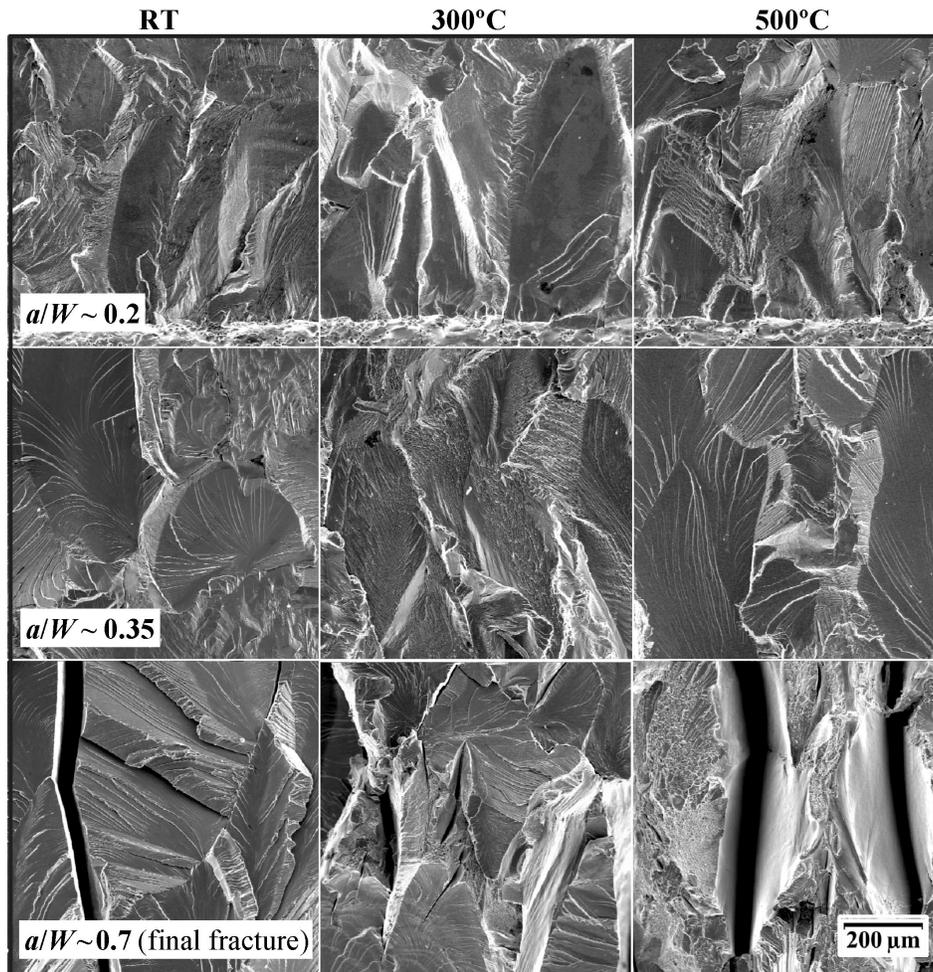
Fig. 2. Fracture surfaces at room temperature (RT) and at elevated temperatures (300, 500 ℃) at the start of the fatigue crack growth (near the pre-crack, $a/W \sim 0.2$), during the fatigue crack growth ($a/W \sim 0.35$) and in the area of final fracture ($a/W \sim 0.7$).

with increasing temperature in the zone of final fracture (Figs. 7 and 8). Fracture mechanism changed from transgranular cleavage at RT to ductile dimpled fracture at 500 ℃. Area of final fracture contained many large intergranular cracks oriented perpendicularly to the fracture surface (significantly in excess of the number of the intergranular cracks found on the fatigue fracture surface). The opening of these intergranular cracks also grows with increasing temperature (Fig. 2).
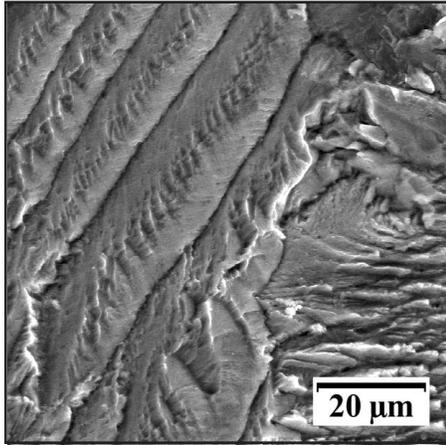
Fig. 3. The interaction of the fatigue crack with dislocation networks (RT).
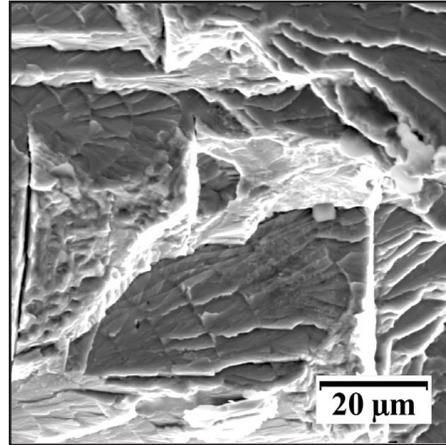
Fig. 4. Cyclic cleavage on fracture surfaces at room temperature.
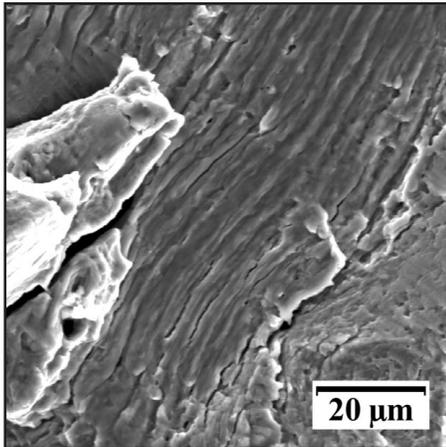
Fig. 5. Ductile striations formed on the fracture surface at 300 °C.
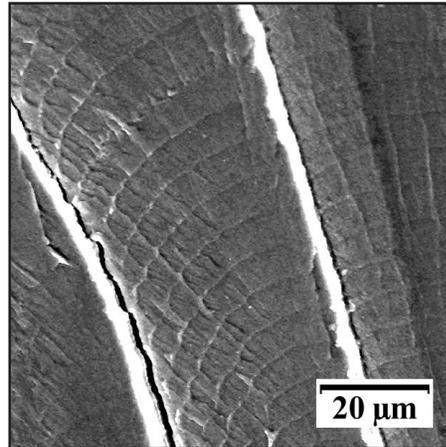

Fig. 6. Brittle striations covering the cleavage facets at 500 °C.

4. Summary

The fatigue crack growth rate (ν-ΔK) curves of the hot rolled Fe-28at.%Al intermetallic alloy with the addition of chromium and cerium were measured at RT, 300 and 500 °C. The alloy presents the best resistance against the fatigue crack growth at 300 °C, except for the low values of $\Delta K (< 24$ MPa $\sqrt{m}$) for which the alloy has the lowest crack growth rate at RT. At 500 °C the slope in ν-ΔK plot
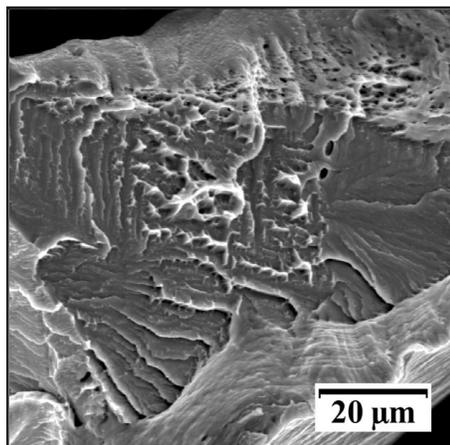
Fig. 7. Signs of increasing plastic deformation during the final fracture at 300 °C.
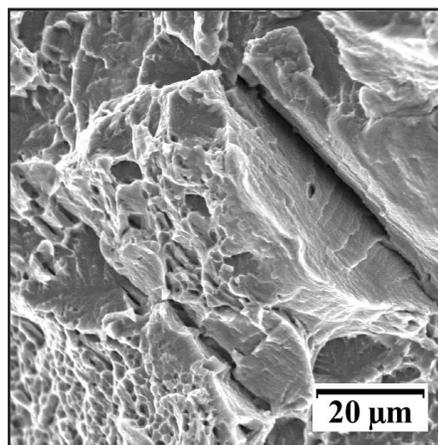
Fig. 8. Ductile dimples on the final fracture surface at 500 °C.

remains practically the same as at 300 °C but the curve is shifted towards the higher crack growth rate values.

The main fatigue crack growth micromechanism is transgranular cleavage at all studied temperatures. Besides transgranular cleavage, transgranular quasi-cleavage facets, ductile fatigue striations and brittle striations were also found on fatigue fracture surfaces. The presence of striations fields on fracture surfaces of tested specimens proves the increase of plastic deformation at the crack tip (crack blunting) in the studied alloy.

In the zone of final (static) fracture, the material showed an increasing capacity of plastic deformation with increasing temperature. Fracture mechanism changed from transgranular cleavage at 20 °C to ductile dimpled fracture at 500 °C.

Acknowledgements

REFERENCES

[1] McKAMEY, C. G.—De VAN, J. H.—TORTORELLI, P. F.—SIKKA, V. K.: J. Mater. Res., *6*, 1991, p. 1779.
[2] WESTBROOK, J. H.—FLEISCHER, R. L. (Eds.): Intermetallic Compounds. New York, John Wiley 1995.
[3] LIU, C. T.—LEE, E. H.—McKAMEY, C. G.: Scripta Metall. Mater., *23*, 1989, p. 875.
[4] DEEVI, S. C.—SIKKA, V. K.: Intermetallics, *4*, 1996, p. 357.

[5] McKAMEY, C. G.—HORTON, J. A.: Metall. Trans., *A20*, 1989, p. 751.
[6] McKAMEY, C. G.—LIU, C. T.: Scripta Metall., *24*, 1990, p. 2219.
[7] YANGSHAN, S.—ZHENGJUN, Y.—ZHONGHUA, Z.—HAIBO, H.: Scripta Metall. Mater., *33*, 1995, p. 811.
[8] HUANG, Y. D.—YANG, W. Y.—CHEN, G. L.—SUN, Z. Q.: Intermetallics, *9*, 2001, p. 331.
[9] HOTAŘ, A.—KRATOCHVÍL, P.: Kovove Mater., *40*, 2002, p. 45.
[10] KRATOCHVÍL, P.—ŠEDIVÁ, I.—HAKL, J.—VLASÁK, T.: Kovove Mater., *40*, 2002, p. 124.
[11] STOLOFF, N. S.: Mater. Sci. Eng., *A258*, 1998, p. 1.
[12] CASTAGNA, A.—STOLOFF, N. S.: Mater. Sci. Eng., *A192/193*, 1995, p. 399.
[13] ALVEN, D. A.—STOLOFF, N. S.: Scripta Mater., *34*, 1996, p. 1937.
[14] ALVEN, D. A.—STOLOFF, N. S.: Mater. Sci. Eng., *A239-240*, 1997, p. 362.
[15] KARLÍK, M.—NEDBAL, I.—SIEGL, J.—PRAHL, J.: J. Alloys Comp. (in press).
[16] KRATOCHVÍL, P.—KARLÍK, M.—HAUŠILD, P.—CIESLAR, M.: Intermetallics, *7*, 1999, p. 847.
[17] KARLÍK, M.—KRATOCHVÍL, P.—JANEČEK, M.—SIEGL, J.—VODIČKOVÁ, V.: Materials Science and Engineering, *A289*, 2000, p. 182.
[18] NEDBAL, I.—SIEGL, J.—KUNZ, J.: In: Proceedings of ICF 7, Houston. Vol. *5*. Oxford, Pergamon Press 1989, p. 3483.